MAGNETIC RESONANCE IN CHEMISTRY
Magn. Reson. Chem. 2006; **44**: S122–S129
Published online in Wiley InterScience (www.interscience.wiley.com). DOI: 10.1002/mrc.1819

Dipolar dynamic frequency shifts in multiple-quantum spectra of methyl groups in proteins: correlation with side-chain motion

Vitali Tugarinov,[1] Jason E. Ollerenshaw[1,2] and Lewis E. Kay[1]*

[1] Departments of Medical Genetics, Biochemistry and Chemistry, University of Toronto, Toronto, Ontario, M5S 1A8, Canada
[2] Ontario Cancer Institute and Department of Medical Biophysics, University of Toronto, 610 University Avenue, Toronto, Ontario, M5G 2M9, Canada

Received 22 November 2005; Revised 19 January 2006; Accepted 28 February 2006

Small deviations from the expected relative positions of multiplet components in double- and zero-quantum ^{1}H-^{13}C methyl correlation maps have been observed in spectra recorded on a 7-kDa protein. These dynamic frequency shifts (DFS) are the result of dipolar cross-correlations that derive from fields produced by the spins within the methyl groups. The shifts have been quantified and compared with values calculated from a Redfield analysis. Good agreement is noted between the signs of the predicted and experimentally observed relative shifts of lines in both F_1 and F_2 dimensions of spectra, as well as between the magnitudes of the calculated and observed shifts in the F_2 (^{1}H) dimension. The experimental DFS values show a reasonable correlation with ^{2}H relaxation-derived measures of methyl side-chain dynamics, as expected from theory. This suggests that in cases where such shifts can be quantified, they can serve as qualitative measures of motion. Copyright © 2006 John Wiley & Sons, Ltd.

KEYWORDS: dynamic frequency shift; multiple-quantum spectroscopy; methyl group; cross-correlated relaxation; side-chain order parameter

INTRODUCTION

Over the past several decades cross-correlated spin relaxation has been exploited by NMR spectroscopists as a valuable probe of molecular dynamics and structure.[1–4] In addition to providing important insight into motional processes and information about structure, such effects can also be used to improve both the resolution and the sensitivity of certain experiments when applied to macromolecules, via transverse relaxation optimized spectroscopy or TROSY.[5] In both types of application, a description of the underlying physics can be obtained within a framework that considers the decay properties of NMR signals. These decay properties, in turn, depend on cosine Fourier transforms of time-dependent angular functions that describe the orientation of magnetic interactions with respect to the laboratory frame.[6] However, time-dependent perturbation theory establishes that in addition to these terms, there are related expressions that derive from sine Fourier transforms of the corresponding angular functions that contribute in second order to shifts of resonance frequencies.[6] In principle, such terms that account for these so called dynamic frequency shifts[7–9] (DFS) also contain information about molecular dynamics.

Experimental and theoretical studies of DFS of spin-1/2 nuclei coupled to quadrupolar spins have been published,[10–13] showing that cross-correlation effects between dipolar and quadrupolar interactions can have a dramatic effect on the spin-1/2 multiplet pattern. These effects can be substantial (e.g. for a $^{13}C-^{2}H$ spin-system the central carbon line shift is of the order of 6 Hz in the slow-motion limit at 600 MHz) and are readily observed in terms of an asymmetry in the multiplet structure. In the case of pairs of spin-1/2 particles, such as $^{15}N-^{1}H$ spin systems attached to macromolecules such as proteins, dipolar/chemical shift anisotropy interference gives rise to small shifts in multiplet components, of the order of several tenths of a hertz, that can be quantified.[14,15] These effects are of particular importance in the context of the measurement of residual dipolar couplings in molecules that are aligned via magnetic susceptibility anisotropy because they are of similar size to the couplings themselves.[14]

The relaxation properties of transitions in degenerate spin systems such as those in methyl groups are significantly influenced by cross-correlated dipole–dipole interactions.[16] Dynamic frequency shifts have been calculated for degenerate spin-1/2 A_3 systems and are predicted to result in a separation of the degenerate multiplet components.[17] Dynamic frequency shifts of ^{13}C multiplet components of methanol dissolved in glycerol have been observed experimentally in 1D spectra.[18] Here, too, the measured shifts were very small, although somewhat larger than the predicted values.

In principle, the same process that leads to the observation of DFS in 1D ^{13}C spectra of methyl groups in small

*Correspondence to: Lewis E. Kay, Departments of Medical Genetics, Biochemistry and Chemistry, University of Toronto, Toronto, Ontario, M5S 1A8, Canada.
E-mail: kay@pound.med.utoronto.ca

molecules dissolved in viscous solvents should also produce shifts of methyl multiplet components in 2D $^{1}H-^{13}C$ correlation maps. Here we show, with an application to a small protein in which all multiplet components can be observed, that indeed this is the case. Dynamic frequency shifts have been measured in both F_1 and F_2 dimensions of $^{1}H-^{13}C$ double-quantum (DQ) and zero-quantum (ZQ) quantum methyl spectra of a small protein, protein L (64 residues).[19] Although the magnitudes of the shifts in the multiplet patterns observed in both DQ and ZQ spectra are small, the signs of such shifts are in agreement with predictions based on theory; notably the degeneracy of the ^{1}H transitions is lifted, with individual ^{1}H lines separated by as much as 0.4 Hz. Calculations show that these dynamic frequency shift values report directly on the amplitudes of motion of the methyl threefold axis and, indeed, a reasonable agreement is obtained between measured shifts and order parameters that have been quantified for methyl groups in protein L by ^{2}H spin relaxation methods.[20,21]

EXPERIMENTAL

NMR sample

A {U-[^{15}N, ^{2}H], Ile δ1-[$^{13}CH_3$], Leu, Val-[$^{13}CH_3$, $^{12}CD_3$]}-labeled sample of the B1 immunoglobulin binding domain of peptostreptoccocal protein L[19] was prepared as described previously.[22] The NMR sample was 1.4 mM in protein, 99.9% D_2O, 50 mM sodium phosphate buffer, pH 6.0 (uncorrected).

NMR spectroscopy

NMR experiments were performed on 500 and 600 MHz Varian Inova spectrometers equipped with pulsed-field gradient triple resonance probes. Sensitivity enhanced $^{1}H-^{13}C$ spectra were recorded using a scheme that is very similar to that published previously,[23] with the exception that in this case a pair of data sets was recorded in an interleaved manner. In the first data set, coherences evolve as the sum of $^{1}H-^{13}C$ ZQ and DQ during t_1 ($2C_x \sum_i H_x^i$, where A_i is the i component of A magnetization and the summation is over all three methyl protons), while in the second the difference (ZQ-DQ, $2C_y \sum_i H_y^i$) is recorded. Data matrices comprising [380(320),512(512)] complex points were recorded in (t_1, t_2) at 500(600) MHz, corresponding to acquisition times of 211(211) and 64(64) ms, respectively (^{2}H decoupling was not employed in either t_1 or t_2). Linear combinations of the data sets were generated in a postacquisition manner to produce separate DQ and ZQ maps that were subsequently transformed to yield spectra with cross-peaks centered (F_1) at $\Omega_C + \Omega_H$ (DQ) and $\Omega_C - \Omega_H$ (ZQ), where $\Omega_C(\Omega_H)$ is the carbon(proton) offset from the carrier.

All NMR spectra were processed with the programs NMRPipe/NMRDraw.[24] Extensive zero-filling was used in both t_1 and t_2 to produce a final data set size of $8\,K \times 8\,K$ real points. Slight phase distortions in the F_1 dimensions of the DQ/ZQ spectra (<10°) were corrected by phasing each F_1 trace using the relation: phase $= a + b\Omega_H$. Peak positions were determined by fitting cross-peak contours to elliptical shapes starting at 50% peak intensity, using the interactive peak-picking program PIPP[25] or via parabolic interpolation of intensities in the vicinity of the peak maximum; very similar results were obtained in both cases.

The molecular tumbling correlation time of protein L in D_2O at 25 °C (τ_C = 4.97 ns; assumed isotropic) was obtained from a τ_C value calculated from ^{15}N relaxation measurements performed on samples dissolved in H_2O, as described previously,[21] and subsequently scaled by the ratio of viscosities of D_2O to H_2O at 25 °C. Viscosity ratios can be obtained from tabulated values[26] or experimentally from ratios of translational diffusion constants measured for protein L samples in H_2O and D_2O at 25 °C; ratios from either approach are in quantitative agreement.[22]

The use of a highly deuterated protein, with protonation restricted to Ile δ1 methyls and one of the methyl groups of Leu and Val residues (Leu, Val-[$^{13}CH_3$, $^{12}CD_3$])[27] minimizes cross relaxation between multiplet components in DQ/ZQ spectra that arise from spin flips involving external protons, as well as contributions to individual lines from long-range scalar couplings. In principle, the (unresolved) splittings that result should not bias the measurements reported here because all lines should be affected equally.

RESULTS AND DISCUSSION

Two-dimensional $^{1}H-^{13}C$ DQ and ZQ spectra of $^{13}CH_3$-labeled Ile, Leu and Val methyl groups in protein L were recorded as described in the Section on Materials and Methods. In these experiments the signal evolves at the frequency $\Omega_C + \Omega_H$ (DQ spectrum) or $\Omega_C - \Omega_H$ (ZQ) during the indirectly detected acquisition period (t_1) and at Ω_H during the direct detection period (t_2), where $\Omega_{C/H}$ is the offset frequency from the carrier for the C/H resonance. The signal is additionally modulated by $\cos^2(\pi {}^{1}J_{CH} t_1)$, where $^{1}J_{CH}$ is the one-bond $^{13}C-^{1}H$ scalar coupling constant leading to triplets in the indirect dimensions (F_1) of both spectra.

It has long been established that, in the macromolecular tumbling limit, the network of cross-correlated dipolar interactions that mediate the relaxation of a $^{13}CH_3$ spin-system divide its SQ and MQ coherences into slowly- and fast-relaxing classes.[16,28–30] With reference to the energy level diagram for an AX_3 spin-system, Fig. 1, the fast-relaxing coherences are those involving the outer states of the $I = 3/2$ manifold (blue), while the slowly relaxing coherences involve transitions between the inner $I = 3/2$ states (red) and within the two $I = 1/2$ manifolds (green). We have shown previously that the type of MQ pulse sequence used here supports two coherence transfer pathways: one involves exclusively fast-relaxing coherences and gives rise to the outer lines of the observed F_1 triplet, while the other involves only slowly relaxing coherences and gives rise to the central line.[31,32] In especially large molecules, the difference between fast and slow relaxation rates is generally so pronounced that only the central line is observable;[31] in applications involving small proteins, such as protein L, all lines are observed, although the effects of differential relaxation of lines are clearly noticeable. With reference to the present work the transitions of interest are denoted in Fig. 1 by arrows; ^{1}H SQ transitions are indicated by vertical arrows while $^{1}H-^{13}C$ DQ and ZQ coherences are depicted by negatively and positively sloping diagonal lines, respectively.

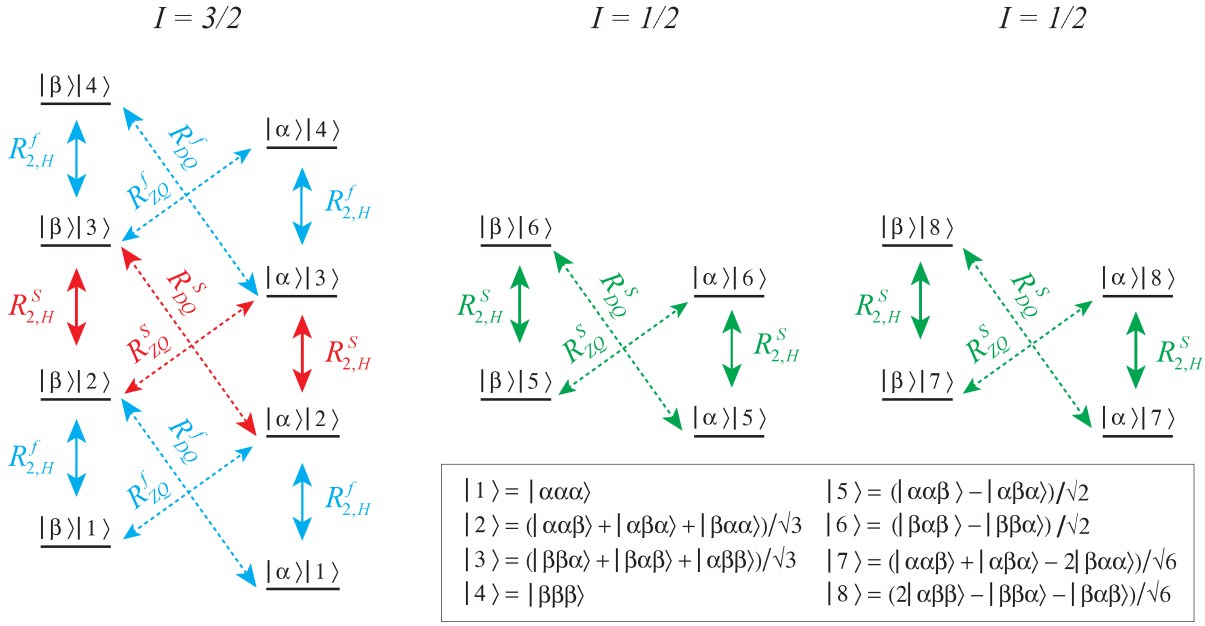

Figure 1. Energy level diagram for an isolated $^{13}CH_3$ spin-system. Eigenfunctions are denoted by $|i\rangle|j\rangle$ where i and j refer to the ^{13}C and ^{1}H spin states, respectively. Vertical lines correspond to ^{1}H single-quantum transitions (F_2 dimension of DQ/ZQ correlation map), while diagonal lines denote double- (negative slope) and zero-quantum (positive slope) transitions (F_1 dimension of DQ/ZQ correlation map). Transitions are color-coded so as to indicate the origin of the correlations in Fig. 2. $R^{S}_{2,H}$ and $R^{f}_{2,H}$ denote slow and fast-relaxing ^{1}H transitions, respectively, while R^{S}_{DQ} and R^{f}_{DQ}(R^{S}_{ZQ} and R^{f}_{ZQ}) are the slow and fast relaxation rates, respectively, of DQ (ZQ) transitions.

In the absence of DFS, all components of the triplet have the same frequency in the ^{1}H dimension (F_2), and the peaks are evenly spaced in F_1 with a separation of $^{1}J_{CH}$. However, the structure of the multiplet becomes more complex when DFS are taken into account, as shown schematically in Fig. 2 for DQ (Fig. 2(a)) and ZQ (Fig. 2(b)) spectra. Such shifts are small but measurable; experimental DQ and ZQ data are illustrated in Fig. 2(c), for a pair of residues (L56 δ2 and L38 δ2). Notably, the outer components in the DQ spectrum are considerably more broadened than their counterparts in the ZQ data set. In fact, both fast and slowly relaxing DQ coherences decay more rapidly than their counterpart ZQ lines due to cross-correlated dipolar interactions involving spins that are external to those that participate in the DQ/ZQ transitions.[23] In what follows, only the relative displacements of multiplet components are considered so that contributions that affect all lines equally can be ignored.

In general, these displacements can be expressed in terms of the imaginary parts of cross-spectral density functions for pairs of dipolar interactions within the methyl group, denoted by $Q^{x}_{\mu\nu}(\omega)$ where μ and ν index the interactions ($\mu \neq \nu$). These spectral densities derive from the underlying cross-correlation functions $C^{x}_{\mu\nu}(t)$ according to

$$Q^{x}_{\mu\nu}(\omega) = \int_0^\infty C^{x}_{\mu\nu}(t)\sin(\omega t)\,dt \qquad (1)$$

and have the following properties:

$$Q^{x}_{\mu\nu}(\omega) = Q^{x}_{\nu\mu}(\omega),\ Q^{x}_{\mu\nu}(-\omega) = -Q^{x}_{\mu\nu}(\omega),\ Q^{x}_{\mu\nu}(0) = 0 \qquad (2)$$

In the context of a methyl group attached to a macromolecule, the model-free formalism of Lipari and Szabo[33,34] can be used to parameterize $Q^{x}_{\mu\nu}(\omega)$ as follows:[30]

$$Q^{x}_{\mu\nu}(\omega) = \frac{1}{5}\left\{S^2_{\text{axis}}S_{\text{axis},\mu}S_{\text{axis},\nu}\frac{\omega\tau_C^2}{1+(\omega\tau_C)^2} + [P_2(\cos\theta_{\mu,\nu}) - S^2_{\text{axis}}S_{\text{axis},\mu}S_{\text{axis},\nu}]\frac{\omega\tau_e^2}{1+(\omega\tau_e)^2}\right\} \qquad (3)$$

where S_{axis} is the order parameter quantifying the amplitude of motions of the methyl threefold axis, $P_2(x) = \frac{1}{2}(3x^2-1)$, $\theta_{\mu,\nu}$ is the angle between the two dipolar interaction vectors, $S_{\text{axis},a} = P_2(\cos\theta_{\text{axis},a})$ with $\theta_{\text{axis},a}$ the angle between the methyl axis and dipolar vector a, τ_C is the correlation time of global molecular reorientation (assumed isotropic), and $\tau_e^{-1} = \tau_f^{-1} + \tau_C^{-1}$ where τ_f is the correlation time for local motions. Note that auto-spectral density functions need not be considered because, in general, DFS induced by auto-correlated relaxation interactions have the same effect on all components of a multiplet,[18] and, therefore, do not contribute to the relative displacements measured in the present work. Although more complex models for $Q(\omega)$ could be constructed this seems unwarranted given the small relative line shifts observed, and thus the limited precision in extracted DFS (see below).

Dynamic frequency shifts in F_2

Specific relative displacements of lines in the DQ and ZQ spectra of methyl groups will now be considered, concentrating first on shifts in the acquisition dimension. In both DQ and ZQ experiments, the outer lines of the F_1 triplet move downfield (to higher frequency) in F_2 relative to the central line because of ^{1}H–^{1}H dipolar DFS, predicted in an earlier study by Werbelow and coworkers.[17] These shifts

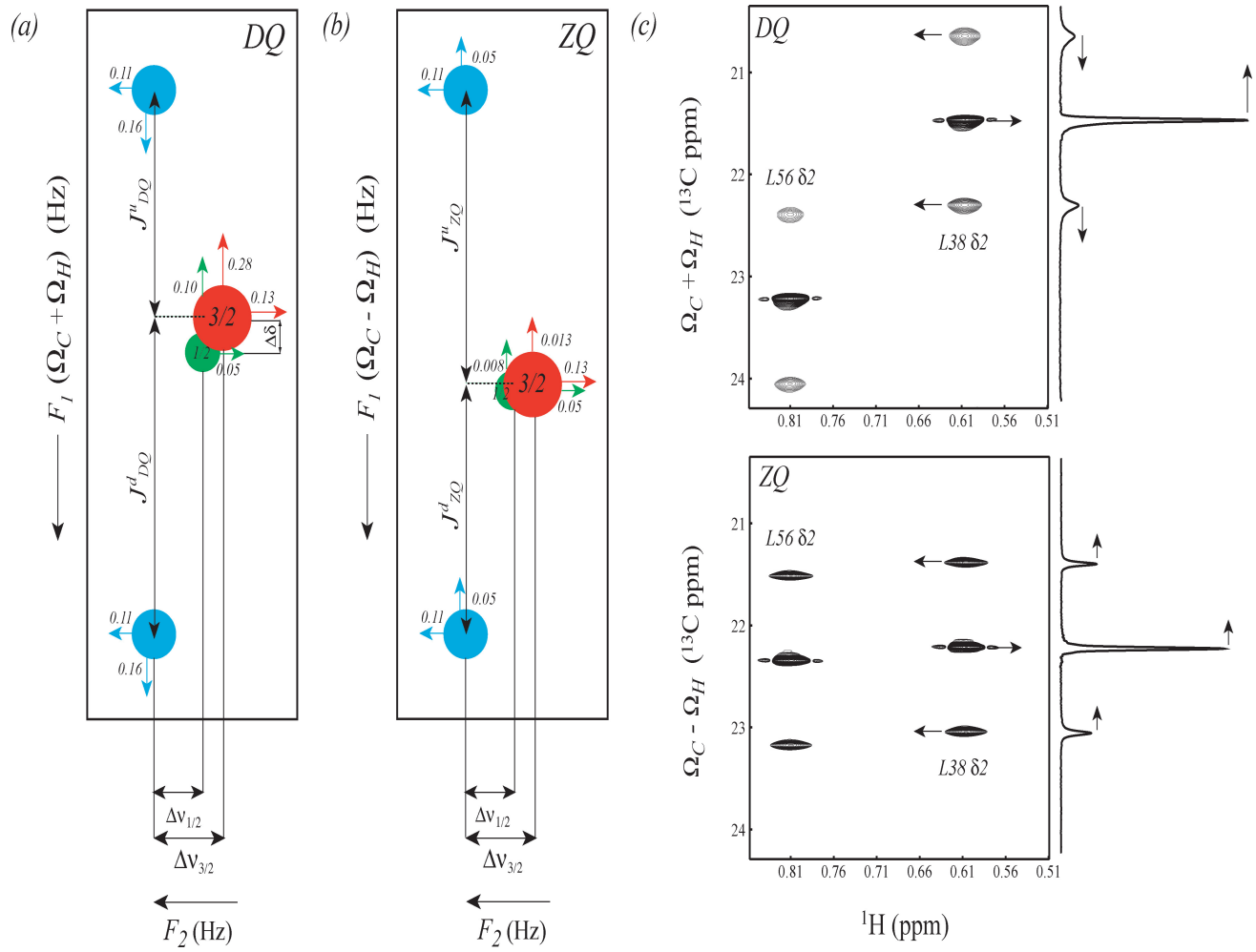

Figure 2. Schematic representation of relative displacements of multiplet components in (a) ^{1}H–^{13}C DQ and (b) ^{1}H–^{13}C ZQ spectra of methyl groups due to cross-correlated dipolar relaxation interactions (so called dynamic frequency shifts). Frequency separations between the centers of peaks are labeled using the symbols adopted in this work. Red circles represent central components of the triplet that derive from the $I = 3/2$ manifold of the AX_3 spin-system, and specifically from the transitions labeled with red arrows in Fig. 1, while green circles represent central components associated with the two $I = 1/2$ manifolds, deriving from the transitions in green in Fig. 1. The outer components of the multiplets are shown with blue circles and result from the transitions indicated in blue in Fig. 1 ($I = 3/2$ manifold). The shifts of different components of each of the triplets are highly exaggerated for clarity, and their displacements in both F_1 and F_2 dimensions are indicated with arrows; shifts of each of the lines that result from intra-methyl dipolar cross-correlations only are listed for the dynamics parameters ($\tau_C = 4.97$ns, $S^2_{axis} = 0.52$, $\tau_f = 40$ps), to give the reader an appreciation of the size of the DFS values at 600 MHz. (c) A selected region from ^{1}H–^{13}C DQ (top) and ZQ (bottom) spectra recorded on a highly deuterated, U-[^{15}N,^{2}H], Ileδ1-[^{13}CH$_3$], Leu,Val-[^{13}CH$_3$,^{12}CD$_3$]-labeled sample of protein L, 25 °C (600 MHz). Cross-peaks are positioned in F_1 at the sum (DQ) and difference (ZQ) of offsets of ^{13}C and ^{1}H methyl spins from their respective carriers. For clarity, the frequency labeling in F_1 is recast in terms of ^{13}C ppm values. 1D traces from the F_1 dimensions of DQ and ZQ spectra are shown for the L38 δ2 methyl. Arrows beside peaks in the spectra indicate the directions of relative peak displacements due to DFS in the F_2(^{1}H) dimension, while the arrows shown on 1D traces indicate directions of peak displacements in F_1.

are illustrated as horizontal arrows in Fig. 2. Interestingly, contributions to the central line from coherences within the $I = 3/2$ manifold (red peaks in Fig. 2(a), (b)) are predicted to have different DFS values than contributions from the $I = 1/2$ manifolds (green peaks).[17] The separation in F_2 between the outer lines (blue) and the $I = 3/2$ part of the central line (red), $\Delta\nu_{3/2}$ is given by

$$\Delta\nu_{3/2} = \left\{3d^2_{HH}Q^x_{HH}(\omega_H) - \frac{3}{2}d^2_{HH}Q^x_{HH}(2\omega_H)\right\} \Big/ 2\pi \qquad (4a)$$

with the corresponding separation between the outer lines and the $I = 1/2$ (green) portion of the central line, $\Delta\nu_{1/2}$, given by

$$\Delta\nu_{1/2} = \frac{3}{2}d^2_{HH}Q^x_{HH}(\omega_H) \Big/ 2\pi \qquad (4b)$$

In Eqn (4) $d^2_{HH} = (\mu_0/4\pi)^2\,(6\hbar^2\gamma^4_H/r^6_{HH})$, μ_0 is the vacuum permeability constant, γ_H is the proton gyromagnetic ratio, and r_{HH} is the proton–proton distance in a methyl group. The imaginary part of the ^{1}H–^{1}H dipolar cross-spectral density, $Q^x_{HH}(\omega)$, is given by Eqn (3) with $S_{axis,\mu} = S_{axis,\nu} = -1/2$ and $P_2(\cos\theta_{\mu,\nu}) = -1/8$. Notably, no dipolar interactions involving the ^{13}C nucleus contribute to either $\Delta\nu_{3/2}$ or

$\Delta\nu_{1/2}$, though auto-correlated $^{13}C-^{1}H$ interactions do affect the absolute positions of the multiplet components in F_2. The only other possible contribution to DFS in F_2 would arise from ^{1}H chemical shift anisotropy/$^{1}H-^{1}H$ dipolar cross-correlation interactions. However, this contribution is expected to be negligible since ^{1}H CSA in methyl groups is very small.[35]

The frequency difference in F_2 between the outer and central lines of each observed triplet, $\Delta\nu_{exp}$, has been quantified for 15 Ile ($\delta1$), Leu, Val methyl groups in protein L. Although identical DFS effects in F_2 are predicted for DQ and ZQ spectra, we prefer to analyze the ZQ data since the outer lines are more intense in this spectrum (see discussion above). An average value for $\Delta\nu_{exp}$ of 0.25 ± 0.08 (0.28 ± 0.07) Hz was obtained from ZQ data sets recorded at 500 (600) MHz. We note in passing that in cases where alignment from the anisotropic susceptibility of the protein does occur, differences in the positions of the outer lines would be observed due to dipolar couplings between methyl protons, since each of the outer lines moves in equal but opposite directions, with the central line unaffected. The degree of alignment for protein L is expected to be very small; in fact, the standard deviation in the average absolute frequency differences between the two outer lines of correlations in the 600 MHz ZQ data set is 0.050 Hz. It is noteworthy that $\Delta\nu_{exp}$ has been obtained from the displacement of the central line from the *average position of the two outer lines*, so that any contribution from alignment is eliminated.

For comparison with experimental values of $\Delta\nu_{exp}$, theoretical F_2 frequency differences $\Delta\nu_{3/2}$ and $\Delta\nu_{1/2}$ have been calculated for the same 15 resonances that have been quantified experimentally, using Eqns (3) and (4) with dynamic parameters (τ_f, S^2_{axis}) measured for these methyls in a previous study.[20] The $I = 3/2$ and $I = 1/2$ components of the central line have an average predicted separation, $\Delta\nu_{3/2} - \Delta\nu_{1/2}$, of 0.10 ± 0.03 (0.09 ± 0.03) Hz at 500 (600) MHz, and are, therefore, too close together to be observed as distinct peaks. However, because the $I = 1/2$ component contributes only 1/3 of the total intensity of the central line, and because each peak was fit to an elliptical cross-section at 50% of its height, we assume that the experimentally measured values correspond to $\Delta\nu_{3/2}$. Figure 3 shows the correlation between the calculated ($\Delta\nu_{3/2}$) and experimental ($\Delta\nu_{exp}$) shifts in F_2 at 500 (Fig. 3(a)) and 600 MHz (Fig. 3(b)). Though there are some differences between the theoretical and experimental values, reflecting the limited precision of the measurements, the direction of the displacement is correctly predicted for all the 15 methyl groups studied in protein L.

Dynamic frequency shifts in F_1

In the indirectly detected dimensions of the DQ and ZQ spectra, the correlation for each methyl group is a triplet, with each line separated by the $^{13}C-^{1}H$ coupling constant. Because $^{1}J_{CH}$ cannot be known with absolute precision, only DFS, which perturb the symmetry of the triplet, creating a difference between the two observable spacings are measured. We denote this difference as $[J^d - J^u]$ where $J^{d/u}$ is the splitting on the downfield/upfield side of the triplet (Fig. 2(a), (b)). Using Redfield theory,[36] we have determined that $[J^d - J^u]$ includes contributions from $^{1}H-^{1}H$, $^{13}C-^{1}H$, and $^{13}C-^{1}H/^{1}H-^{1}H$ cross-correlated spectral densities and is given by:

$$[J_d - J_u]^{I=3/2}_{\frac{DQ}{ZQ}} = \{\pm 6d^2_{HH}Q^x_{HH}(\omega_H) \mp 3d^2_{HH}Q^x_{HH}(2\omega_H) + d^2_{CH}Q^x_{CH}(\omega_C) - d^2_{CH}Q^x_{CH}(\omega_H + \omega_C) + \tfrac{1}{6}d^2_{CH}Q^x_{CH}(\omega_H - \omega_C) + 3d^2_{CH,HH}\,Q^x_{CH,HH}(\omega_H)\}/2\pi \quad (5)$$

and

$$[J_d - J_u]^{I=1/2}_{\frac{DQ}{ZQ}} = [J_d - J_u]^{I=3/2}_{\frac{DQ}{ZQ}} - 2\Delta\delta_{\frac{DQ}{ZQ}} \quad (6)$$

where $\Delta\delta_{\frac{DQ}{ZQ}}$, the difference in shifts between the $I = 3/2$ and $I = 1/2$ components of the central line (red and green peaks in Fig. 2(a), (b)) is given by

$$\Delta\delta_{\frac{DQ}{ZQ}} = \{\pm\tfrac{3}{2}d^2_{HH}Q^x_{HH}(\omega_H) \mp \tfrac{3}{2}d^2_{HH}Q^x_{HH}(2\omega_H) - \tfrac{3}{2}d^2_{CH}Q^x_{CH}(\omega_H + \omega_C) + \tfrac{1}{4}d^2_{CH}Q^x_{CH}(\omega_H - \omega_C) + \tfrac{3}{2}d^2_{CH,HH}Q^x_{CH,HH}(\omega_H)\}/2\pi. \quad (7)$$

Note that different values of $[J^d - J^u]$ are predicted for the DQ and ZQ experiments along with different DFS for the $I = 3/2, 1/2$ central line components, just as discussed above for the F_2 dimension. In the expressions above, $d^2_{CH} = (\mu_0/4\pi)^2(6\hbar^2\gamma^2_H\gamma^2_C/r^6_{CH})$, $d^2_{CH,HH} = (\mu_0/4\pi)^2(6\hbar^2\gamma^3_H\gamma_C/r^3_{CH}r^3_{HH})$, γ_C is the gyromagnetic ratio for ^{13}C, r_{CH} is the carbon–proton distance in a methyl group, and the other parameters are as defined previously. $Q^x_{CH}(\omega)$ can be evaluated using Eqn (3) with $S_{axis,\mu} = S_{axis,\nu} = P_2(\cos\theta_{CH,axis})$, $P_2(\cos\theta_{\mu,\nu}) = P_2(P_2(\cos\theta_{CH,axis}))$, and $\theta_{CH,axis}$ is the angle between any of the methyl $^{13}C-^{1}H$ bonds and the methyl threefold axis. Noting that only cross-correlated $^{13}C-^{1}H$ and $^{1}H-^{1}H$ interactions that involve a shared proton contribute to DFS, $Q^x_{CH,HH}(\omega)$ is evaluated with $S_{axis,\mu}S_{axis,\nu} = -0.5P_2(\cos\theta_{CH,axis})$ and $P_2(\cos\theta_{\mu,\nu}) = P_2[-\sqrt{3}\sin(\theta_{CH,axis})/2]$. In all that follows we have used $\theta_{CH,axis} = 110.5°$, $r_{CH} = 1.115$ Å and $r_{HH} = \sqrt{3}\,r_{CH}\sin(\theta_{CH,axis})$.[37,38]

We have evaluated Eqn (5) using a set of typical motional parameters describing the dynamics of Ile($\delta1$), Leu and Val methyl groups in protein L ($\tau_C = 4.97$ ns, $S^2_{axis} = 0.52$, $\tau_f = 40$ps),[20] and obtained values of 1.04 (0.88) Hz and – 0.104 (–0.074) Hz for $[J^d - J^u]^{I=3/2}_{DQ}$ and $[J^d - J^u]^{I=3/2}_{ZQ}$, respectively, at 500 (600) MHz. Notably, the terms describing $^{1}H-^{1}H$ cross-correlations (first two terms in Eqn (5)) account for approximately half of the total value of $[J^d - J^u]^{I=3/2}_{DQ}$. Because these terms change in sign between the DQ and ZQ cases, the theoretical value of $[J^d - J^u]^{I=3/2}_{ZQ}$ is much smaller than $[J^d - J^u]^{I=3/2}_{DQ}$ and has the opposite sign. The theoretically predicted F_1 displacements of spectral components in DQ and ZQ spectra of methyl groups are shown schematically in Fig. 2(a), (b) and qualitatively as vertical arrows in Fig. 2(c). For the same motional parameters listed above, $[J^d - J^u]^{I=1/2}_{DQ}$ and $[J^d - J^u]^{I=1/2}_{ZQ}$ are calculated to be 0.64 (0.53) Hz and – 0.102 (–0.084) Hz at 500 (600 MHz), respectively, while $\Delta\delta = 0.18$ (0.005) Hz for the DQ (ZQ)

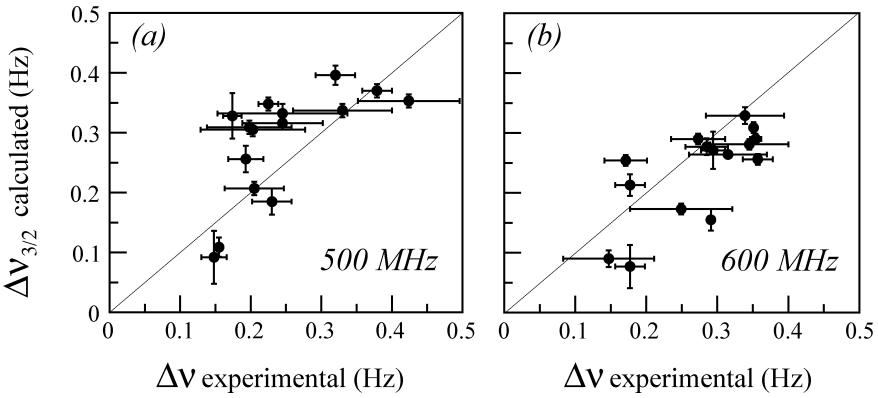

Figure 3. Correlation plots between calculated, $\Delta\nu_{3/2}$, (y-axis) and experimental, $\Delta\nu$, (x-axis) values measured from ^{1}H–^{13}C ZQ methyl spectra of protein L at (a) 500 MHz and (b) 600 MHz. Calculated values have been obtained using Eqns (3) and (4a), along with (S^2_{axis}, τ_f) values determined previously from ^{2}H relaxation experiments recorded on protein L at 25 °C.[20] Values of bond lengths and angles used are as listed in the text.

experiment at 600 MHz. This frequency difference ($\Delta\delta$) is too small for the components to be observed experimentally as separate peaks. As described above, because the contribution to the central line from the $I = 3/2$ manifold is twice that from the $I = 1/2$ manifold, in what follows comparisons of experimental values of $[J^{\text{d}} - J^{\text{u}}]$ will be made with the calculated $[J^{\text{d}} - J^{\text{u}}]^{I=3/2}$ values.

Experimental observations confirm the predicted asymmetry of F_1 triplets in the DQ and ZQ spectra of methyl groups in protein L. Careful measurements of the upfield and downfield splittings in the 500 (600) MHz data sets yield average experimental values of $[J^{\text{d}} - J^{\text{u}}]_{\text{DQ}} = 1.56 \pm 0.50$ (2.25 ± 0.55) and $[J^{\text{d}} - J^{\text{u}}]_{\text{ZQ}} = -0.16 \pm 0.06$ (-0.28 ± 0.07) Hz, over the set of 13 Ile(δ1), Leu and Val methyl resonances that could be quantified. These values are consistent with the above theoretical considerations in that $[J^{\text{d}} - J^{\text{u}}]_{\text{DQ}} > 0$, $[J^{\text{d}} - J^{\text{u}}]_{\text{ZQ}} < 0$, and $|[J^{\text{d}} - J^{\text{u}}]_{\text{DQ}}| > |[J^{\text{d}} - J^{\text{u}}]_{\text{ZQ}}|$. However, it is apparent that Eqn (5) significantly underestimates the magnitude of the experimentally observed shifts. On average, the experimental values of $|[J^{\text{d}} - J^{\text{u}}]_{\text{DQ}}|$ and $|[J^{\text{d}} - J^{\text{u}}]_{\text{ZQ}}|$ exceed the theoretically predicted values by factors of 1.6 and 3.7, respectively. At this time we cannot explain these discrepancies, nor why the displacements measured in F_1 are larger at 600 MHz than at 500 MHz. However, it is worth noting that the derivations in this work all assumed an isolated methyl group and a simple motional model (Eqn (3)). In addition, from a practical perspective, quantification of small shifts is extremely sensitive to phasing artifacts that could introduce systematic errors.[14] It is of interest to note that in their studies of DFS effects in methanol dissolved in glycerol, Werbelow and coworkers could account for only a portion of the observed shifts using a theoretical analysis similar to that reported here.[18]

Finally, we wish to emphasize that the $[J^{\text{d}} - J^{\text{u}}]_{\text{DQ/ZQ}}$ differences quantified in this work are purely dipolar in origin. While ^{13}C CSA/^{13}C–^{1}H dipolar cross-correlations can contribute to DFS, such interactions do not affect the position of the central line of each F_1 triplet, and shift the outer lines equally in opposite directions, leaving $[J^{\text{d}} - J^{\text{u}}]_{\text{DQ/ZQ}}$ unchanged. The shifts from residual dipolar couplings are similar to those due to CSA/dipolar interactions and are therefore also subtracted out by taking the difference $[J^{\text{d}} - J^{\text{u}}]$. Also, note that the DFS displacements predicted here for the DQ spectrum are qualitatively similar to those observed in the spectra of a spin-1/2 nucleus coupled to a spin-1 particle (e.g. a ^{13}CD triplet).[10–12]

Correlations with side-chain motion

To investigate the sensitivity of the DFS effects described above to methyl group dynamics, we have calculated $\Delta\nu_{3/2}$ and $[J^{\text{d}} - J^{\text{u}}]^{I=3/2}_{\text{DQ/ZQ}}$ values as a function of S^2_{axis} (Fig. 4(a)) and τ_f (Fig. 4(b)). For a given value of τ_f the dependence of $\Delta\nu_{3/2}$ and $[J^{\text{d}} - J^{\text{u}}]^{I=3/2}_{\text{DQ/ZQ}}$ on S^2_{axis} is linear (Fig. 4(a) with $\tau_f = 40$ ps). Values of $\Delta\nu_{3/2}$ and $[J^{\text{d}} - J^{\text{u}}]^{I=3/2}_{\text{DQ/ZQ}}$ are only weakly dependent on τ_f over the range of τ_f values found by ^{2}H spin relaxation studies[20] of Ile(δ1), Leu, Val methyl groups in protein L (20–80 ps; Fig. 4(b)). In contrast to the values of $[J^{\text{d}} - J^{\text{u}}]^{I=3/2}_{\text{DQ}}$ that are always positive for the parameters considered in the simulations reported here, the values of $[J^{\text{d}} - J^{\text{u}}]^{I=3/2}_{\text{ZQ}}$ are predicted to pass through zero and change sign as τ_f increases (Fig. 4(b)), due to the compensation between DFS contributions that are purely ^{1}H–^{1}H dipolar in origin and those that depend on ^{13}C–^{1}H dipolar interactions (Eqn (5)). However, for all Ile, Leu, Val methyls quantified in protein L, only negative $[J^{\text{d}} - J^{\text{u}}]_{\text{ZQ}}$ values were observed.

It is noteworthy that in the macromolecular limit ($\omega\tau_{\text{C}} \gg 1$) there is only a relatively weak dependence of measured shifts on τ_{C}. For example, in applications involving protein L at 25 °C, $(\omega_{\text{C}}\tau_{\text{C}})^2 \sim 20$ (600 MHz) so that the spectral density function of Eqn (3) is essentially independent of τ_{C}. Thus, an accurate determination of molecular diffusion parameters, whereas critical in studies of protein dynamics by relaxation rate measurements, becomes less important in applications that involve DFS values. However, this gain is moderated by the small magnitude of the DFS effects (at least for coupled spin-1/2 systems) and by the fact that as τ_{C} increases, some of the lines that are required for measurement of $[J^{\text{d}} - J^{\text{u}}]$ values become very weak or disappear altogether.

Figure 5 shows correlation plots relating ^{2}H-derived methyl axis order parameters squared, S^2_{axis}, and $[J^{\text{d}} - J^{\text{u}}]_{\text{DQ}}$ (Fig. 5(a)) and $[J^{\text{d}} - J^{\text{u}}]_{\text{ZQ}}$ (Fig. 5(b)) measured at 600 MHz.

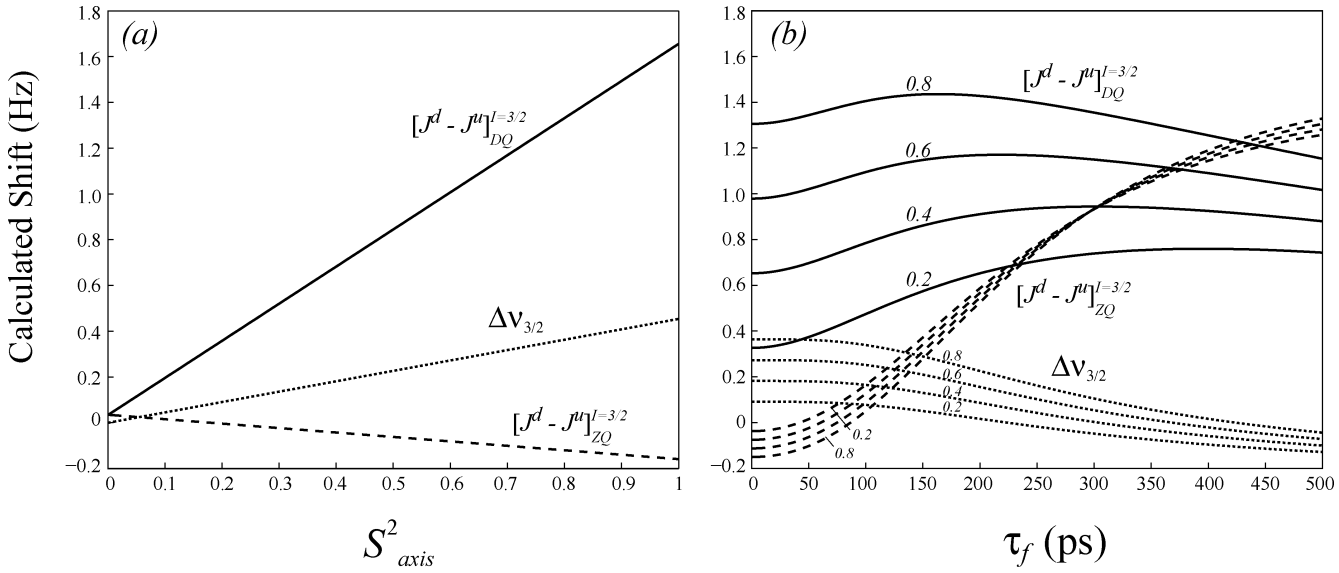

Figure 4. Calculated dependence of $\Delta\nu_{3/2}$ (dotted curves), $[J^d - J^u]^{I=3/2}_{DQ}$ (solid curves) and $[J^d - J^u]^{I=3/2}_{ZQ}$ (dashed curves) on (a) methyl axis order parameter squared, S^2_{axis}, and (b) local motion correlation time, τ_f. The plots in (a) have been generated using $\tau_f = 40$ ps. The plots in (b) are calculated for the S^2_{axis} values of 0.2, 0.4, 0.6 and 0.8 covering the range of all Ile δ1, Leu and Val S^2_{axis} values in protein L. All plots have been calculated assuming $\tau_C = 4.97$ ns, bond lengths and angles given in the text, and a 600 MHz spectrometer field.

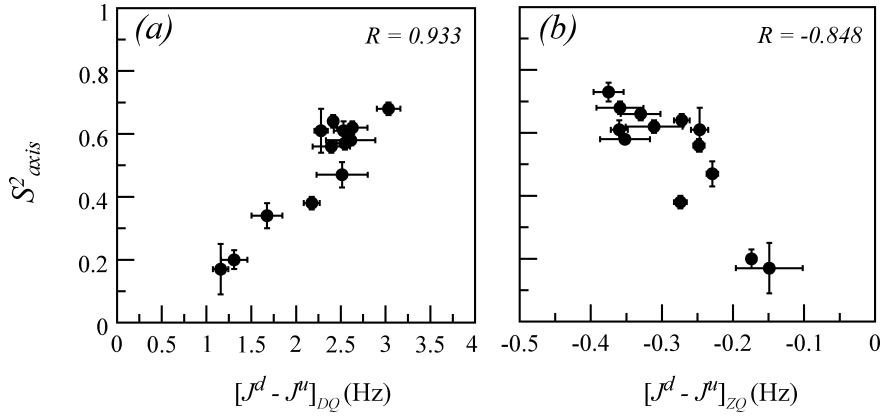

Figure 5. Correlation plots between methyl axes order parameters squared, S^2_{axis}, derived from ^{2}H spin relaxation measurements on a fractionally deuterated, ^{13}C-labeled protein L sample at 25 °C,[20] *y*-axis, and (a) experimental values of $[J^d - J^u]_{DQ}$ and (b) $[J^d - J^u]_{ZQ}$ measured at 600 MHz, *x*-axis. Pearson correlation coefficients are indicated in the top right corners of the plots. The data is shown for 13 peaks (methyls of Val47 γ2 and Val2 γ1 were excluded from the analysis because of partial overlap). ^{2}H relaxation data for Ile4 δ1, Leu 8 δ1 and δ2 could only be properly fitted with a model that includes nanosecond time-scale dynamics, as described previously.[20] Errors in ^{2}H-derived order parameters are indicated with vertical bars. Random errors in $[J^d - J^u]_{DQ}$ and $[J^d - J^u]_{ZQ}$ (shown with horizontal bars) have been estimated from duplicate measurements (600 MHz). Similar correlations have been obtained from data recorded at a spectrometer field of 500 MHz.

Although the absolute values of the experimental data are significantly higher than predictions from theory (see discussion above) a strong correlation is observed with methyl order parameters. Somewhat worse correlations, $R = 0.66(0.72)$ for data recorded at 500(600) MHz, have been obtained for measured dynamic frequency shift differences, $\Delta\nu$, in the ^{1}H dimension and S^2_{axis} (because $\Delta\nu_{3/2}$ is linearly dependent on S^2_{axis} the plots of Fig. 3(a), (b) essentially illustrate the desired correlation).

In summary, an experimental and theoretical study of DFS in multiple-quantum spectra of $^{13}CH_3$ methyl groups in macromolecules has been presented. Theory correctly predicts many of the noted spectral features that derive from DFS effects, although only a portion of the shifts quantified in the indirect acquisition dimension can presently be accounted for. A reasonable agreement between measured DFS values and methyl S^2_{axis} is noted, confirming expectations based on theory, and underscoring the potential of using DFS as qualitative estimates of the relative flexibility of methyl-containing side-chains in small proteins.

Acknowledgements

This work was supported by a grant from the Canadian Institutes of Health Research (CIHR) to L.E.K., who also holds a Canada Research

Chair in Biochemistry. V.T. and J.E.O. acknowledge postdoctoral fellowships from CIHR and the Alberta Heritage Foundation for Medical Research, respectively. The authors thank Dr V. Kanelis (Hospital for Sick Children, Toronto, Canada) for providing the selectively methyl-labeled sample of protein L.

REFERENCES

1. Werbelow LG, Grant DM. *Adv. Magn. Reson.* 1977; **9**: 189.
2. Vold RL, Vold RR. *Prog. NMR Spectrosc.* 1978; **12**: 79.
3. Schwalbe H, Carlomagno T, Hennig M, Junker J, Reif B, Richter C, Griesinger C. *Methods Enzymol.* 2001; **338**: 35.
4. Dittmer J, Kim CH, Bodenhausen G. *J. Biomol. NMR* 2003; **26**: 259.
5. Pervushin K, Riek R, Wider G, Wüthrich K. *Proc. Natl. Acad. Sci. U.S.A.* 1997; **94**: 12 366.
6. Abragam A. *Principles of Nuclear Magnetism*. Clarendon Press: Oxford, 1961.
7. Werbelow LG. *J. Chem. Phys.* 1979; **70**: 5381.
8. Werbelow LG, London RE. *Conc. Magn. Reson.* 1996; **8**: 325.
9. Brüschweiler R. *J. Chem. Phys.* 1996; **105**: 6164.
10. Grzesiek S, Bax A. *J. Am. Chem. Soc.* 1994; **116**: 10 196.
11. London RE, LeMaster DM, Werbelow LG. *J. Am. Chem. Soc.* 1994; **116**: 8400.
12. Werbelow LG, London RE. *J. Chem. Phys.* 1995; **102**: 5181.
13. Gabel SA, Luck LA, London RE, Werbelow LG. *J. Magn. Reson.* 1997; **128**: 101.
14. Tjandra N, Grzesiek S, Bax A. *J. Am. Chem. Soc.* 1996; **118**: 6264.
15. Desvaux H, Kummerle R, Kowalewski J, Luchinat C, Bertini I. *Chemphyschem* 2004; **5**: 959.
16. Werbelow LG, Marshall AG. *J. Magn. Reson.* 1973; **11**: 299.
17. Werbelow LG, Thevand A, Pouzard G. *J. Chem. Soc., Faraday Trans. 2* 1979; **75**: 971.
18. Chenon MT, Dunkel R, Grant DM, Werbelow LG. *J. Phys. Chem.* 1999; **103**: 1447.
19. Scalley ML, Yi Q, Gu H, McCormack A, Yates JR, Baker D. *Biochemistry* 1997; **36**: 3373.
20. Skrynnikov NR, Millet O, Kay LE. *J. Am. Chem. Soc.* 2002; **124**: 6449.
21. Millet O, Muhandiram DR, Skrynnikov NR, Kay LE. *J. Am. Chem. Soc.* 2002; **124**: 6439.
22. Tugarinov V, Kay LE. *J. Biomol. NMR* 2004; **29**: 369.
23. Tugarinov V, Sprangers R, Kay LE. *J. Am. Chem. Soc.* 2004; **126**: 4921.
24. Delaglio F, Grzesiek S, Vuister GW, Zhu G, Pfeifer J, Bax A. *J. Biomol. NMR* 1995; **6**: 277.
25. Garrett DS, Powers R, Gronenborn AM, Clore GM. *J. Magn. Reson.* 1991; **95**: 214.
26. Cho CH, Urquidi J, Singh S, Robinson GW. *J. Phys. Chem. B* 1999; **103**: 1991.
27. Tugarinov V, Kay LE. *J. Biomol. NMR* 2004; **28**: 165.
28. Müller N, Bodenhausen G, Ernst RR. *J. Magn. Reson.* 1987; **75**: 297.
29. Kay LE, Prestegard JH. *J. Am. Chem. Soc.* 1987; **109**: 3829.
30. Kay LE, Torchia DA. *J. Magn. Reson.* 1991; **95**: 536.
31. Tugarinov V, Hwang PM, Ollerenshaw JE, Kay LE. *J. Am. Chem. Soc.* 2003; **125**: 10 420.
32. Ollerenshaw JE, Tugarinov V, Kay LE. *Magn. Reson. Chem.* 2003; **41**: 843.
33. Lipari G, Szabo A. *J. Am. Chem. Soc.* 1982; **104**: 4559.
34. Lipari G, Szabo A. *J. Am. Chem. Soc.* 1982; **104**: 4546.
35. Tugarinov V, Scheurer C, Brüschweiler R, Kay LE. *J. Biomol. NMR* 2004; **30**: 397.
36. Redfield AG. *IBM J. Res. Dev.* 1957; **1**: 19.
37. Ishima R, Petkova AP, Louis JM, Torchia DA. *J. Am. Chem. Soc.* 2001; **123**: 6164.
38. Ottiger M, Bax A. *J. Am. Chem. Soc.* 1999; **121**: 4690.